MAGNETOHYDRODYNAMICS Vol. 51 (2015), No. 3, pp. 419–424

APPLICATION OF MAGNETICALLY DRIVEN TORNADO-LIKE VORTEX FOR STIRRING FLOATING PARTICLES INTO LIQUID METAL

I. Grants, D. Räbiger, T. Vogt, S. Eckert, G. Gerbeth

Helmholtz-Zentrum Dresden-Rossendorf, Bautzner Landstr. 400, 01328 Dresden, Germany

A tornado-like liquid metal vortex is driven by magnetic body forces. A continuously applied rotating magnetic field provides a source of the angular momentum. A pulse of a much stronger travelling magnetic field drives a converging flow that temporarily focuses this angular momentum towards the axis of the container. A highly concentrated vortex forms that produces a funnel-shaped surface depression. The ability of this vortex to entrain floating unwetted particles in liquid metal is investigated experimentally.

Introduction. The magnetic bar stirrer is a useful piece of standard laboratory equipment. It creates a whirlpool that somewhat resembles a tornado [1] and efficiently entrains floating powder into the liquid. The mechanics of such a flow is largely based on a simple principle. Due to angular momentum conservation, the circular motion of a fluid accelerates towards the center of a converging flow. Such converging and spinning liquid metal flow may be generated by alternating magnetic fields in a fully contactless way. A converging flow may be created by the travelling magnetic field (TMF). The angular momentum, in turn, can be injected by the rotating magnetic field (RMF). To avoid interference of both fields, their frequencies should be considerably different [2, 3]. At certain conditions when the TMF induced magnetic force is about 100 times stronger than the RMF force, this combination produces a quasi-steady concentrated vortex [2] that somewhat resembles atmospheric vortices. This vortex, however, remains blurred and does not develop a pronounced funnel on the surface. It appears not nearly as effective in entraining floating particles as the magnetic bar stirrer vortex. During the spin-up phase, however, a reproducible sharp deep vortex funnel is observed. The difference from the established flow is explained by a relatively low level of turbulence during the spin-up [4] that enables a much higher degree of vortex concentration.

The aim of the current experiment is to assess suitability of such transient flow for the purpose of stirring floating particles into the melt. If successful, such approach may be used in the technology of metal matrix composite casting as well as for rapid contactless insertion of buoyant alloying elements or reagents in the metal bulk.

1. Background.

1.1. Magnetic forces. Let us consider a liquid metal cylinder of diameter $2R_0$ with constant electric conductivity σ, kinematic viscosity ν and density ρ inserted in uniform rotating and travelling magnetic fields with flux densities $B_{\mathrm{R,T}}$ and angular frequencies $\omega_{\mathrm{R,T}}$, respectively. The axial wave number of TMF is κ. Under the common low-frequency and low-induction conditions, the RMF and TMF induce magnetic body forces with the well-known distribution [2]. The RMF induces a purely azimuthal force, whose time-averaged value is given by

$$F_\phi = \sigma\omega_{\mathrm{R}} B_{\mathrm{R}}^2 r f(r,z), \tag{1}$$

where $f(r, z)$ is a dimensionless shape function of the radial and axial coordinate, respectively. This force drives a rotating flow with secondary meridional circulation [5]. The dimensionless force magnitude is given by the magnetic Taylor number

$$\mathrm{Ta} = \frac{\sigma\omega_{\mathrm{R}} B_{\mathrm{R}}^2 R_0^4}{\rho\nu^2}. \tag{2}$$

The TMF creates an axially directed force, whose time-averaged value is given by [2]

$$F_z = 0.25\sigma\omega_{\mathrm{T}} B_{\mathrm{T}}^2 \kappa r^2. \tag{3}$$

Depending on the direction of the TMF wave vector, the liquid metal at the outer part of the container is pushed up- or downwards that drives an axisymmetric flow torus. The dimensionless magnitude of this force is

$$F = \frac{\sigma\omega_{\mathrm{T}} B_{\mathrm{T}}^2 \kappa R_0^5}{2\rho\nu^2}. \tag{4}$$

The magnetic flux density of both magnetic fields B_{R} and B_{T} in Eqs. (1) and (3), respectively, is given in terms of the root mean square value. The magnetic force expressions (1, 3) assume a low frequency of the respective alternating magnetic field. This is true if the shielding factor

$$S = \mu_0 \sigma\omega_{\mathrm{T}} R_0^2 < 3, \tag{5}$$

where μ_0 is the magnetic permeability [5]. This is fulfilled in our experiment.

2. Properties of the transient tornado-like vortex. A pulse of a strong upwards directed TMF initiates a converging flow at the top surface. Because of the angular momentum conservation the azimuthal velocity attains a $\propto 1/r$ profile in the outer inviscid part of this converging flow. Being strong enough, the flow produces a surface deformation on the metal surface. Depending on the RMF strength, the deformation has the shape of a single sharp funnel or multiple smaller depressions rotating about a common centre (Fig. 4 in Ref. [4]). This flow pattern is robust and reproducible during the initial spin-up only. As flow matures, the funnel breaks down. There are two distinct regimes controlled by the strength of the RMF. For a weak RMF, the peak swirl is much weaker than the TMF driven meridional flow and it increases with Ta while the vortex width stays invariant. For a strong RMF, the peak swirl intensity stays nearly constant approaching that of the meridional flow velocity while the vortex diameter increases with Ta. The maximum swirl concentration is, thus, reached on the border between those regimes at a certain "optimum" RMF strength $\mathrm{Ta}_{\mathrm{tr}}$. This threshold value is a function of the TMF intensity F and depends strongly on the type of boundary conditions at the top surface. For a free top surface, $\mathrm{Ta}_{\mathrm{tr}}/F \propto F^{-0.625}$ while for a solid cover $\mathrm{Ta}_{\mathrm{tr}}/F \propto F^{-0.4}$ (Fig. 12b in Ref. [4]).

3. Experiment.

3.1. Magnetic system. The inductor of combined magnetic fields KOMMA [6] was used (see Fig. 1). At the bottom of the inductor bore there is a built-in cooling plate for directional solidification. The inductor is designed for the generation of RMF and TMF, whereby the field parameters $B_{\mathrm{R}}, B_{\mathrm{T}}, \omega_{\mathrm{R}}$ and ω_{T} can be controlled independently. The generation of the RMF is realized by a radial arrangement of six coils, whereby opposing coils are connected as pole-pairs. The TMF is generated inside a line-up of six coils at an equal distance of $h = 0.035\,\mathrm{m}$, yielding a wave number of $\kappa = 2\pi/6h = 30\,\mathrm{m}^{-1}$. The frequency of the RMF is fixed to $\omega_{\mathrm{R}}/2\pi = 50\,\mathrm{Hz}$ and the TMF frequency is $\omega_{\mathrm{T}}/2\pi = 100\,\mathrm{Hz}$ in this study. The

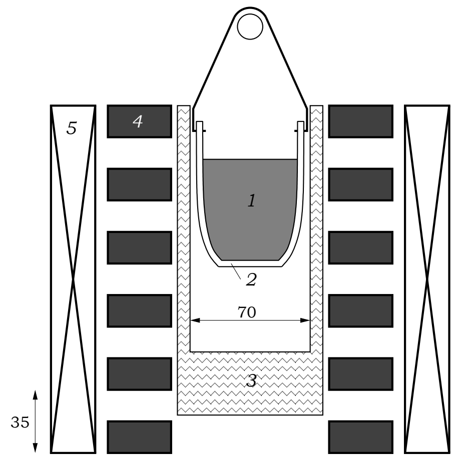

Fig. 1. Scheme of the experiment with sizes given in mm. *1* – molten metal; *2* – ceramic crucible; *3* – water cooled jacket; *4* – TMF coils; *5* – RMF coils.

diameter of the inductor's bore is 70 mm. The TMF coils are fed by a three-phase alternating current from three power amplifiers coupled to high current transformers. That allows to minimize the ramp-up time of the TMF pulse to a few milliseconds.

3.2. Particle insertion procedure. Tin is molten and overheated to 320°C in a ceramic quartz crucible of 50 mm in diameter. The height of the molten metal is about 50 mm. Floating oxides and other impurities are mechanically removed from the surface. The crucible is then inserted into the inductor, with the RMF continuously running. After about 30 s, the TMF pulse is applied and simultaneously the particles (45 μm diameter Al_2O_3 spheres) are dropped on the surface. The duration of the TMF pulse is 2 s. Such pulses are then periodically repeated every 10 s until the metal solidifies.

3.3. Estimates of the magnetic field strength. Formation of a sharp surface depression has been observed [4] for a value of the dimensionless parameter

$$\mathscr{F} = \frac{\sigma\omega_{\mathrm{T}} B_{\mathrm{T}}^2 R_0^2}{2(\rho g s)^{1/2}} \kappa R_0 = F \frac{\nu^2}{g h_{\mathrm{c}} R_0^2} > 3, \qquad (6)$$

where $h_{\mathrm{c}} = (\gamma/\rho g)^{1/2} \approx 2.5$ mm is the capillary length, g is the gravity acceleration and γ is the surface tension. To be on the safe side, let us choose $\mathscr{F} = 10$ that produces $F \approx 1.6 \times 10^8$ for tin. The magnetic field induction can now be estimated as $B_{\mathrm{T}} = 75$ mT at $\omega_{\mathrm{T}}/2\pi = 100$ Hz for a $2R_0 = 50$ mm container. The following physical properties of liquid tin are assumed: $\rho = 7 \times 10^3$ kg/m^3, $\sigma = 2 \times 10^6$ S/m, $\nu = 10^{-6}$ m^2/s and $\gamma = 0.5$ N/m. Depending on the boundary conditions on the top surface, the calculated optimum RMF strength $\mathrm{Ta}_{\mathrm{tr}}$ varies between 7×10^4 ($B_{\mathrm{R}} \approx 1.4$ mT) for free-slip and 53×10^4 ($B_{\mathrm{R}} \approx 3.9$ mT) for no-slip [4].

4. Results and discussion. The oxide layer is quickly formed on the surface of the molten tin creating an uncertainty in the boundary conditions, which strongly influences the optimum RMF induction. Therefore, we first observed the surface deformation without adding particles.

The oxide layer turned out to be rigid enough to resist the initial RMF driven flow. However, the layer was broken by the spin-up vortex shortly after the beginning of the TMF pulse. The pulse only caused a significant surface deformation (see Fig. 2), when the RMF strength was at the upper limit of estimates $B_{\mathrm{R}} \approx 4$ mT,

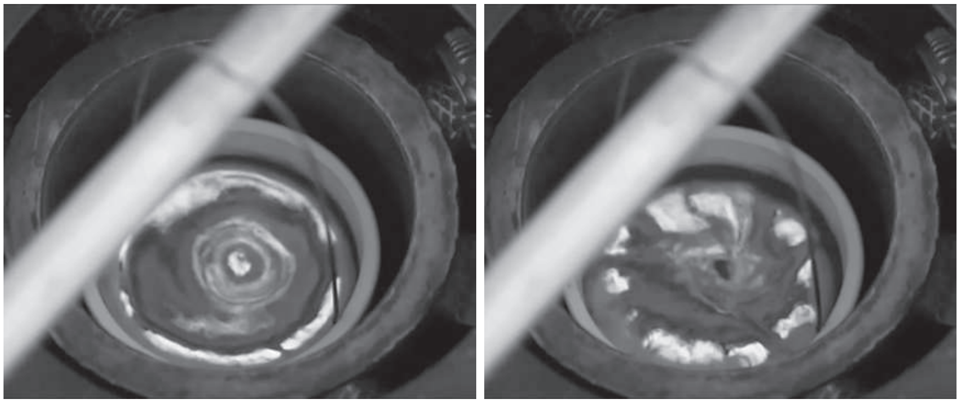

(*a*) (*b*)

Fig. 2. Surface of molten tin (*a*) 0.27 s and (*b*) 0.40 s after the beginning of the TMF pulse; $B_{\mathrm{T}} = 75\,\mathrm{mT}$, $B_{\mathrm{R}} = 4\,\mathrm{mT}$.

corresponding to the "optimum" for the no-slip boundary conditions. That shows that the boundary conditions influence the spin-up vortex basically through the initial conditions. In case of free-slip, the upper layer of the initial flow carries considerably more angular momentum than in case of no-slip. The role of the boundary conditions appears limited to the initial state, since the shift to nearly free-slip conditions during the spin-up phase did not reduce the "optimum" RMF.

The spin-up funnel had a duration of about 0.25 to 0.3 seconds that is considerably shorter than in [4]. This difference was basically due to a smaller container. Substituting the experimentally and numerically observed correlation for the dimensionless spin-up time $\tau = 9F^{-1/2}$ [4] in Eq. (6) with the value $\mathscr{F} = 10$ one obtains that the corresponding dimensional spin-up time

$$\tau^* = \frac{R_0^2}{\nu}\tau \approx \frac{3R_0}{(gh_{\mathrm{c}})^{1/2}} \tag{7}$$

scales linearly with the container size. The capillary lenght turns out to be the single material property influencing the duration of the spin-up funnel. This expression produces $\tau^* = 0.47\,\mathrm{s}$ that with account for the funnel formation time of $\approx 0.2\,\mathrm{s}$ agrees well with the observed funnel duration. The top speed of the vortex is limited by the maximum axial velocity attained at the end of the spin-up. In dimensionless terms, this velocity is approximated by the correlation $v_z = 1.7F^{1/2}$ [4]. Expressing now F from Eq. (6) with $\mathscr{F} = 10$, it follows that the characteristic velocity is an invariant of the container size,

$$v_z^* = \frac{\nu}{R_0}v_z \approx 5(gh_{\mathrm{c}})^{1/2}, \tag{8}$$

that corresponds to 0.8 m/s in our experiment.

Although short-lived, the funnel was able to entrain a sizable part of particles dropped on the surface at the beginning of the pulse. The submerged particles, however, popped out of the metal immediately after the TMF pulse. Apparently, they formed a "pocket" that did not fragment in the turbulent flow following the funnel collapse. This behavior might have been caused by an oxide film enwrapping the particles. Another cause could be an insufficient level of turbulence due to the small size of the crucible. Repeated pulses gradually reduced the amount of the floating particles on the surface. However, after the solidified ingot was removed from the crucible, it turned out that most particles accumulated at the crucible wall just beneath the surface of metal.

The oxide film may be prevented by an appropriate flux. The flux, however, will wet the oxide particles and, thus, hold them trapped. This may be avoided by the following approach. In another attempt to stir the particles into the melt, we alloyed them mechanically with tin into pellets. For this purpose, we mixed one part of aluminum oxide particles with five parts by mass of tin powder (45 μm). The powder mixture was then mechanically pressed into 8 mm thick discs. The density of these disks was 5.2 kg/m^3 that implies a porosity of about 20%. The discs were cut into pieces of a characteristic size of 4 mm. The pellets (30 g) were dropped on the surface of the melt at the beginning of the TMF pulse. The spin-up vortex entrained and kept them submerged for the entire duration of the pulse. A lesser part of the pellets appeared on the surface after the pulse. The sample was solidified under a continuous TMF with a reduced flux density of $B_{\mathrm{T}} = 25$ mT. Some of the submerged pellets were found at the side edge of the solidified ingot. Apparently, they have been held pressed to the crucible wall by surface tension forces. Fig. 3 shows four microscopic views in random locations on the axial cut of the obtained ingot. By counting individual particles in eight such micrographs, the average inter-particle distance is estimated as 0.45 mm. That corresponds to a particle volume fraction of 0.05% at most. Thus, no more than 5% of the particles initially in the pellets were mixed into the metal. This poor performance is likely

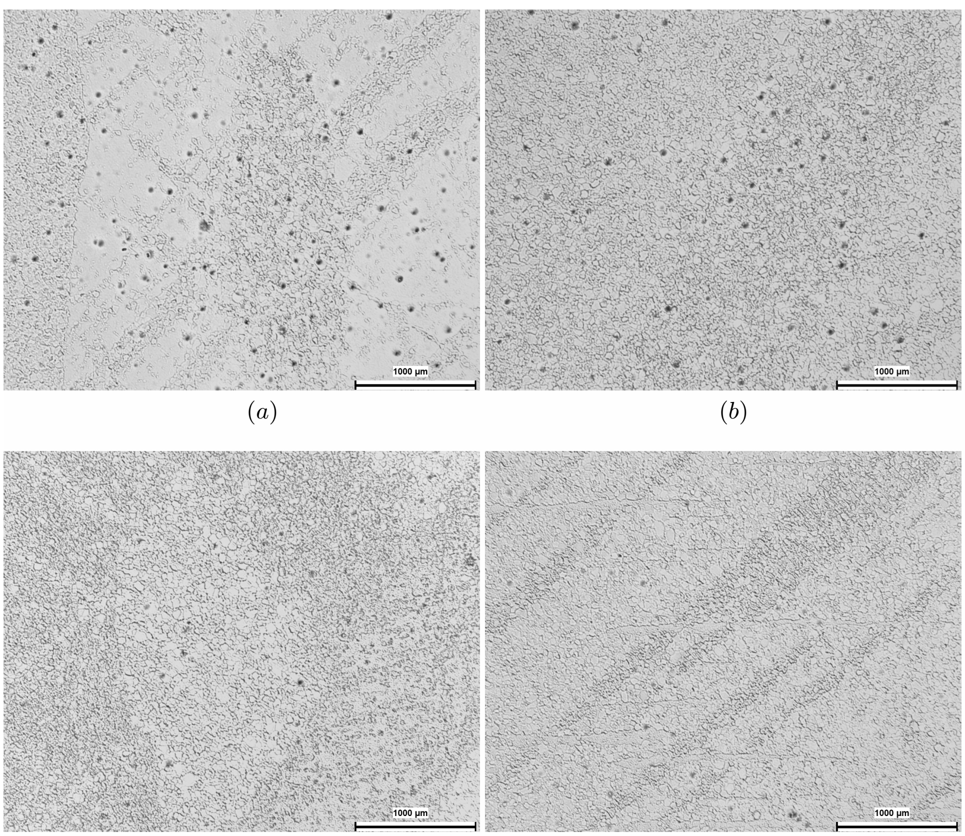

(*a*) (*b*) (*c*) (*d*)

Fig. 3. Microscopic view of selected sections with the largest (*a*),(*b*) and the smallest (*c*),(*d*) number of Al_2O_3 inclusions. The frame area is 12.5 mm^2.

connected to the persistence of pellets even when continuously submerged. The melting time of a pellet with a radius r_{p} is estimated as

$$r_{\mathrm{p}}^2\rho\Lambda/(\Delta T\lambda) \ll 10\,\mathrm{s}, \tag{9}$$

where $\Lambda = 59\,\mathrm{kJ/kg}$ is the heat of fusion and $\lambda \approx 50\,\mathrm{W/Km}$ is the heat conductivity of tin. Thus, the metal contained in pellets should have been molten during the TMF pulse. Apparently, the pellets were held together by capillary forces forming a mixture of microscopic liquid tin droplets, ceramic particles and gas voids. That would not happen if each separate particle was fully enveloped by metal. Thus, a reduced porosity and increased metal volume fraction in the pellets may facilitate their disintegration.

5. Summary. The experiment confirms the condition $\mathscr{F} > 3$ for the formation of a funnel-shaped central depression near the surface of the liquid metal cylinder. The duration of the vortex is consistent with the numerical results in [4]. Provided that $\mathscr{F}$ is kept constant, the funnel duration scales linearly with the size of the container. Floating oxide particles are submerged into liquid metal by the vortex lasting just a fraction of a second. Yet, the particle pocket survives the high velocity flow in our experiment with a relatively small melt volume. The efficiency of particle dispersion may improve in a larger container, where both the funnel duration and the turbulence level should increase. Initial mechanical alloying with the metal facilitates the particle dispersion, which still remains poor in the current test. It is suggested that the surface protection by flux and the use of pellets with a lower porosity and a lower ceramic particle content may improve the efficiency of their dispersion.

Acknowledgements. Samples were kindly prepared by Mrs. M. Rossner from the Division of Structural Materials at Helmholtz-Zentrum Dresden-Rossendorf. Financial support from the Helmholtz Association in form of the Alliance "Liquid Metal Technologies" is gratefully acknowledged.

REFERENCES

[1] G. Halász, B. Gyüre, I.M. Jánosi, K.G. Szabó, T. Tél. Vortex flow generated by a magnetic stirrer. *American J. Phys., vol. 75* (2007), pp. 1092–1098.

[2] I. Grants, C. Zhang, S. Eckert, G. Gerbeth. Experimental observation of swirl accumulation in a magnetically driven flow. *J. Fluid Mech.,* vol. 616 (2008), pp. 135–152.

[3] A. Cramer, J. Pal, G. Gerbeth. Experimental investigation of a flow driven by a combination of a rotating and a traveling magnetic field. *Phys. Fluids*, vol. 19 (2007) 118109.

[4] T. Vogt, I. Grants, S. Eckert, G. Gerbeth. Spin-up of a magnetically driven tornado-like vortex. *J. Fluid Mech.,* vol. 736 (2013), pp. 641–662.

[5] P.A. Davidson. Swirling flow in an axisymmteric cavity of arbitrary profile driven by a rotating magnetic field. *J. Fluid Mech.,* vol. 254 (1992), pp. 669–699.

[6] B. Willers, S. Eckert, P. Nikrityuk, D. Rabiger, J. Dong, K. Eckert, G. Gerbeth. Efficient melt stirring using pulse sequences of a rotating magnetic field: Part II. Application to solidification of Al-Si alloys. *Metall. & Mat. Trans. B*, vol. 39B (2008), pp. 304–316.

Received 24.11.2014